Published in final edited form as:
Mol Cancer Res. 2021 November 01; 19(11): 1957–1969. doi:10.1158/1541-7786.MCR-21-0171.

ADGRL4/ELTD1 expression in breast cancer cells induces vascular normalisation and immune suppression

Helen Sheldon[#1], **Esther Bridges**[#1], **Ildefonso Silva**[#1], **Massimo Masiero**[2], **David M. Favara**[1], **Dian Wang**[2], **Russell Leek**[2], **Cameron Snell**[2], **Ioannis Roxanis**[3], **Mira Kreuzer**[1], **Uzi Gileadi**[4], **Francesca M. Buffa**[1], **Alison Banham**[2], **Adrian L. Harris**[1]

[1]Cancer Research UK Molecular Oncology Laboratories, Weatherall Institute of Molecular Medicine, University of Oxford, John Radcliffe Hospital, Oxford, United Kingdom

[2]Nuffield Division of Clinical Laboratory Sciences, Radcliffe Department of Medicine, John Radcliffe Hospital, Headington, Oxford OX3 9DU, UK

[3]Department of Cellular Pathology, Oxford University Hospitals NHS Foundation Trust, John Radcliffe Hospital, Oxford OX3 9DU, UK

[4]MRC Human Immunology Unit, MRC Weatherall Institute of Molecular Medicine, University of Oxford, John Radcliffe Hospital, Oxford, United Kingdom

[#] These authors contributed equally to this work.

Abstract

ELTD1/ADGRL4 expression is increased in the vasculature of a number of tumour types and this correlates with a good prognosis. Expression has also been reported in some tumour cells with high expression correlating with a good prognosis in hepatocellular carcinoma and a poor prognosis in glioblastoma. Here we show that 35% of primary human breast tumours stain positively for ELTD1, with 9% having high expression that correlates with improved relapse free survival. Using immunocompetent, syngeneic mouse breast cancer models we found that tumours expressing recombinant murine Eltd1 grew faster than controls, with an enhanced ability to metastasize and promote systemic immune effects. The Eltd1-expressing tumours had larger and better perfused vessels and tumour-endothelial cell interaction led to the release of pro-angiogenic and immune modulating factors. M2-like macrophages increased in the stroma along with expression of PD-L1 on tumour and immune cells, to create an immunosuppressive microenvironment that allowed Eltd1 regulated tumour growth in the presence of an NY-ESO-1 specific immune response. Eltd1 positive tumours also responded better to chemotherapy which could explain the relationship to a good prognosis observed in primary human cases. Thus, ELTD1 expression may enhance delivery of therapeutic antibodies to reverse the immunosuppression and

Correspondence to: Adrian L. Harris.

Corresponding authour: Professor Adrian L. Harris, Cancer Research UK Molecular Oncology Laboratories, Weatherall Institute of Molecular Medicine, University of Oxford, John Radcliffe Hospital, Oxford, OX3 9DS, adrian.harris@oncology.ox.ac.uk; Tel: +44-1865-222457; Fax: +44-1865-222431.

Conflict of interest: The authors declare no potential conflicts of interest.

Implications: ELTD1 expression in breast tumour xenografts creates an immunosuppressive microenvironment and increases vessel size and perfusion. Its expression may enhance the delivery of therapies targeting the immune system.

Europe PMC Funders Author Manuscripts

increase response to chemotherapy and radiotherapy in this subset of tumours. ELTD1 may be useful as a selection marker for such therapies.

Keywords

ELTD1 breast cancer immune suppression

Europe PMC Funders Author Manuscripts

Introduction

ELTD1/ADGRL4 is an orphan adhesion G protein coupled receptor (GPCR) and its expression was first identified in smooth muscle cells and cardiomyocytes(1) and then in the normal endothelial transcriptome(2,3). It has an important role in angiogenesis(4,5) and higher ELTD1 expression is associated with the vasculature of a number of tumour types such as ovarian, renal, head and neck, hepatocellular carcinoma and colorectal cancer(4,6). Increased vessel expression in these tumours also correlates with a good prognosis in patients receiving anti-cancer therapies(4,6). *Eltd1* silencing in vessels by intravenous injection of *Eltd1* siRNA reduced the growth of ovarian and colorectal tumour xenografts and reduced metastasis(4). This correlated with a reduced vessel density and is consistent with its pro-angiogenic role. ELTD1 expression has also been described in tumour cells of head and neck, renal, colorectal, glioblastoma and hepatocellular cancers with expression correlating to a good prognosis in hepatocellular carcinoma and to a poor prognosis in glioblastoma(6,7). Previously published studies on the effects of ELTD1 expression in tumour cells have been carried out using human cell lines expressing the human ELTD1 protein(6–9). *In vitro*, overexpression increased the migration and invasiveness of the cells but decreased the *in vivo* growth of hepatocellular tumour xenografts(6) and increased the growth of gliomas(7). The extracellular domain (ECD) of human ELTD1 contains an EGF and a EGF-Ca^{2+} binding repeat, but it is classified within the Latrophilin-like family based on its seven transmembrane region homology(10). These ECD domains are typically found in the ADGRE subfamily of adhesion GPCRs, which are involved in the modulation of immune cell function(11), and these EGF domains might me important as some have been identified as ligand-binding domains(12). The ECDs of mouse and human ELTD1 have only 59% homology and the mouse protein sequence has an extra EGF-Ca^{2+} binding domain. Because if these differences the human ELTD1 sequence may not be able to fully interact with the host stroma in mice and might stimulate a host immune response, potentially explaining some of the inconsistencies seen in previously published data. To investigate the interaction of ELTD1 between tumour cells and the surrounding stroma, particularly in immune response, we expressed the murine Eltd1 sequence in mouse breast tumour cell lines and employed immune competent mouse models to study tumour growth, metastasis and response to systemic therapy.

Materials and Methods

Cell culture and reagents

E0771 (ATCC) were cultured in RPMI supplemented with 10% FBS. 4T1 cells (ATCC), 4T1-NY-ESO-1 (a kind gift from Uzi Gileadi, Oxford), 4T1 expressing GFP (4T1-GFP)

and murine endothelial cells (sEnd-1) (13) were cultured in DMEM supplemented with 10% FBS. Cell lines were authenticated using mouse STR profiling (ATCC) and tested for Mycoplasma contamination (MycoAlert™, Lonza). All media components were purchased from ThermoFisher. Mouse codon optimised *Eltd1* (mcoEltd1) was cloned into pLVX-Puro (Addgene) and the vector alone was used as a control. Virus was produced in 293T cells and the viral supernatant was used to make stable cell lines after selection in 1μg/ml puromycin (ThermoFisher).

Spheroid growth and invasion assay

5000 cells were seeded into round bottomed plates with 2.5% Matrigel™ (BD Biosciences) and centrifuged to form a pellet. The spheroids were photographed at 4x magnification every 24hrs using an AMG Evos XL Core digital microscope (Fisher Scientific). The spheroid area was quantified using Fiji (ImageJ). E0771 cells do not form monolayers therefore invasion was monitored in spheroids. Spheroids were taken after 72hrs and embedded in 50% Matrigel™ (BD Biosciences) and images acquired as described above.

Co-culture experiments

sEnd.1 and 4T1-GFP control or 4T1-GFP-mcoEltd1 cells were mixed 50:50 in 6 well plates and cultured for 48hrs in DMEM supplemented with 2% FCS. After incubation the media was centrifuged and stored at -20°C. Cells were either lysed in TRI Reagent® (Sigma) according to manufacturer's instructions or in 0.5ml of RIPA (Sigma). For FACs sorting experiments, cells were co-cultured as previously described then harvested and separated into 4T1 tumours cells (GFP+) and sEnd.1 endothelial cells (GFP-) using a BD FACSAria cell sorter (BD Biosciences) before lysis in TRI Reagent® (Sigma). For co-culture without physical contact, 4T1-GFP cells were seeded in 6 well plates and an equal number of sEnd.1 cells were seeded into ThinCert™ 6-well culture inserts (Greiner, 1μm, 657610) and the cells co-incubated for 48hrs. Fluorescent images were acquired and quantified using the IncuCyte® Zoom live cell analysis system (Sartorius).

Mouse cytokine array

An equal volume of cell media obtained from co-culture experiments was used in a Proteome Profiler Mouse XL Cytokine array (R&D Systems, ARY028) according to the manufacturer's instructions. Spot intensity was quantified using Fiji.

Syngeneic mouse models

All animal procedures were carried out in accordance with the UK Home Office Licence 30/3197. Mammary fat pad (MFP) models: 100μl of Matrigel™ (BD Biosciences) containing $1x10^6$ E0771 or $2x10^5$ 4T1 mouse breast tumour cells (control and mcoEltd1-expressing), were inoculated into the MFP of wild-type C57BL/6 female mice or BALBc WT female mice aged 5-6weeks respectively. Tumours were measured at least three times a week.

Lung metastasis models—100μl of $1x10^6$ E0771 cells or $1x10^5$ 4T1s mouse breast cells in PBS (control or mcoEltd1-expressing), with or without mcoEltd1, were injected

intravenously into wild-type C57BL/6 female mice or BALBc WT female mice aged 5-6weeks respectively. Animal welfare was monitored daily until endpoint (7 days following tumour inoculation for E0771 and 10 days for 4T1s).

Endpoint procedures—Hypoxyprobe/Pimonidazole (2mg/kg) and a 647-Tomato lectin (1mg/kg)/Hoescht (2mg/kg) mix was given intravenously 5min before *in vivo* fluorescence imaging of perfused tumours/organs visualisation on an *in vivo* imaging system (IVIS™, PerkinElmer), after which the mice were culled.

Isolation of cells from tissues and FACs analysis

Cell isolation protocols were adapted from a Springer Protocol(14). Briefly, tumours were harvested at endpoint and dissociated using collagenase/dispase (Sigma-Aldrich) according to manufacturer's instructions. Spleen cell suspensions were obtained by dissociation through a 70μm cell filter. All cells were treated with red blood cell lysis buffer (ThermoFisher) then counted. Single cell suspensions were stained with different fluorophore-conjugated antibodies (Biolegend). Antibodies used were; anti-CD19 (clone 6D5), anti-CD3 (clone 17A2), anti-CD45 (clone 30-F11), anti-Ly-6C (clone HK1.4), anti-Ly-6G (clone 1A8), anti-F4/80 (clone BM8), anti-CD11b (clone M1/70), anti-CD11b (clone M1/70), anti-CD11c (clone N418), anti-MHC II (clone M5/114.15.2), anti-CD8b (clone YTS156.7.7), anti-CD19 (clone 6D5), anti-NK-1.1 (clone PK136), anti-CD4 (clone GK1.5), anti-CD8a (clone 53-6.7), anti-CD206 (clone C068C2). Flow cytometry was performed using a FACSAria II (BD Biosciences), where 50,000-100,000 events were acquired. All analysis involved automatic compensation before sample acquisition, using the AbC™ Total Antibody Compensation Bead Kit (ThermoFisher). During data acquisition, debris and doublets were excluded. Data obtained were analyzed with the FlowJo software version 5.0 (TreeStar).

IFNγ assay

Mice were injected with 4T1-NY-ESO-1 tumour cells expressing mcoEltd1 or control. A group of naïve/healthy mice were used as control. After 22 days the spleens were collected as described above to detect the presence of specific T CD8+ cells raised against the tumour NY-ESO-1 antigen. The splenocytes (10^6) were stimulated with irrelevant peptide (Flu NP, 1μg/ml) or the NY-ESO-1 peptide (1μg/ml) for 4 h and the T CD8 IFNγ producing cells were quantified by FACS. A positive control for IFNγ production was made by the treating cells with PMA- PMA (10nM)/Ionomycin. After washing, cells were stained with the following antibodies; CD8-APC (clone 53-6.7), CD19-APC Cy7 (clone 6D5), CD44 Brilliant Violet 241 (clone IM7), IFNγ-PE (clone XMG1.2) (all from Biolegend) and LIVE/DEAD™ Aqua (ThermoFisher). After further washing FACS was performed as previously above.

Immunohistochemistry

Human breast tumour samples were obtained in accordance with the National Research Ethics Service South Central Oxford B Research Ethics Committee (project reference number C02.216). Deidentified samples were accessed through the Oxford Centre for Histopathology Research according to UK regulatory requirements.

IHC on primary human tissues—ELTD1 staining was performed using an anti-human ELTD1 antibody (Ab; HPA025229 from Sigma-Aldrich). In brief, paraffin-embedded slides were de-waxed and antigen retrieved by microwaving in 50mM Tris-2mM EDTA (pH 9.0). Sections were incubated with the Ab (1:500; about 1μg/ml) at room temperature for 45 minutes. Bound Ab was detected using the Envision system (DAKO), visualized by using 2,3- diaminobenzidine chromogen and counterstained with haematoxylin. The intensity of ELTD1 staining in tumour and vessels was scored (0=negative, 1=low, 2=moderate, 3=high) by a pathologist.

IHC on xenografts—IHC analysis for cell proliferation (Ki67, M7240; 1:100, Qigent), microvessel density (Endomucin, ab106100, 1:50, Abcam), hypoxia (Hypoxyprobe/ Pimonidazole injection before sacrifice), pericytes (alpha smooth muscle actin, A2547; 1:200, Sigma). Slides were dewaxed and antigen retrieval performed in pH 6. Endogenous peroxidase activity was blocked before slides were stained for 1h at room temperature. Slides were stained using the FLEX staining kit (Agilent) and visualised using 3,3′-Diaminobenzidine (Flex-DAB) chromogen and counterstained with haematoxylin.

Expression of markers and viable/necrotic areas were quantified on whole sections quantitatively by using the Visiopharm Integrator System. HDAB-DAB colour deconvolution band is used to detect positively stained cells. Threshold classification is used to identified necrosis and living regions and thus identify number of positive staining within these regions. Appropriate thresholds levels were checked against control xenografts staining before being set and the xenografts from all groups were then analysed.

Quantitative real-time PCR (QPCR)

Frozen tumours were ground to powder with a pestle and mortar and RNA was extracted using TRI Reagent® (Sigma) according to manufacturer's instructions and reverse transcription was performed using the High Capacity cDNA Archive Kit (Applied Biosystems). Quantitative real time PCR was performed using the SensiFAST™ SYBR No-ROX kit (Bioline) according to the manufacturer's protocols using a RotorGene Q (QIAGEN) The cycling conditions used were: 95 °C for 10 min followed by 40 cycles of 95 °C for 15 s and 60 °C for 60 s. Primers sequences are listed in Supplementary Table 1.

Western blotting

Proteins were separated using by SDS-PAGE using standard techniques. A custom rabbit anti-mouse Eltd1 polyclonal antibody (F04) was generated using an immunogen comprising the three EGF domains of mouse Eltd1 (Cambridge Research Biochemicals), β-actin conjugated to HRP was purchased from Sigma. Secondary antibodies were purchased from DAKO.

Statistics

Prism 8 (Graphpad Software) was used to analyse the results and data shown as mean+/- standard deviation (SD). Student's *t*-test was used to compare two unpaired groups. Kaplan-Meier survival analyses were computed for all survival comparisons. Significance is denoted as: * $p \leq 0.05$, ** $p \leq 0.01$, *** $p \leq 0.001$

Results

Expression of mouse Eltd1 in mouse breast cancer cells does not affect growth *in vitro* but increases tumour size and metastasis *in vivo*

Codon-optimised murine Eltd1 (mcoEltd1) was expressed in the triple receptor negative breast cancer cell line, E0771 (Western blot and QPCR shown in Supplementary Figure 1A). Expression had no significant effect on *in vitro* growth in 2D or 3D culture (Supplementary Figure 1B and 1C) and no significant effect on invasiveness (Supplementary Figure 1D). In a syngeneic C57BL/6 mouse mammary fat pad model, E0771 mcoEltd1 tumours were significantly larger at endpoint (Figure 1A) and were better perfused (Figure 1B and 1C). Increased metastatic burden was also observed in the lungs of mice with mcoEltd1 tumours (spontaneous metastasis formation; Figure 1D, 1E and 1F). IHC of tumour sections revealed an increased size of tumour vessels in the mcoEltd1 tumours compared to the controls (Figure 2A) and an increase in pericyte coverage (Figure 2B) but no significant change in vessel number (Supplementary Figure 2A). There was no difference in overall proliferation (Ki67 staining, Figure 2C) but necrosis (Figure 2D) and Hypoxyprobe/ Pimonidazole staining (Figure 2E) were decreased indicating a reduction in hypoxia.

QPCR confirmed *mcoEltd1* expression in the tumours, as a reliable anti-mouse antibody could not be found for Eltd1 immunohistochemistry (Supplementary Figure 2B). QPCR analysis of RNA extracted from these tumours also showed an increase in endothelial (*Pecam1* and *Cdh5*) and pericyte markers (*Ng2*) confirming the increase in mcoEltd1 tumour vascularity (Supplementary Figure 2C). The use of immune competent mice also allowed us to examine changes in immune cell infiltration and we observed an increase in M2 macrophage markers in the mcoEltd1 tumours compared to controls (Supplementary Figure 2D).

To confirm this growth enhancement, we expressed mcoEltd1 in 4T1 cells which are another mouse triple negative breast cancer cell line. As with the E0771 cells, mcoEltd1 expression had no significant effect on the *in vitro* growth of 4T1 (Supplementary Figure 3A and B) but increased the growth of tumours in a syngeneic BALB/c mouse model with tumours being significantly larger at endpoint (Supplementary Figure 3C). Interestingly, intravenous injection of 4T1 mcoEltd1 cells also resulted in an increased in the number and size of lung metastasis when compared to injection of control cells (Supplementary Figure 3D and E).

Expression of Eltd1 in 4T1 cells enhances their viability in the presence of endothelial cells and modifies the secretome

Eltd1 is an adhesion GPCR and these receptors are thought to function via cell-matrix or cell-cell interactions. Eltd1 is highly expressed in tumour vasculature and, as we observed changes in angiogenesis in mcoEltd1 expressing tumours, we decided to investigate the interaction with endothelial cells *in vitro*. Mouse endothelial cells (sEnd.1) and 4T1-GFP tumour cells were co-cultured for 48hrs and the proliferation of the GFP positive 4T1 cells quantified. 4T1-GFP-expressing mcoEltd1 grew significantly faster than the controls with an 84% increase in cell number (Figure 3A). To establish whether cell-cell contact is required for this effect, cells were co-cultured but separated using ThinCert™ inserts.

4T1-GFP-mcoEltd1 also grew significantly faster than the controls in this setting but to a lesser extent (31% increase; Supplementary Figure 4A). As the effect was greater when the cells physically interacted we used these cells to try to identify factors that could affect cell proliferation. Media was harvested from co-culture experiments after 48hrs and this was used on a Proteome Profiler Mouse XL Cytokine array (R&D Systems). Five factors were found to be significantly increased in the supernatant of mcoEltd1+sEnd.1 co-cultures compared to the controls; Il23, Ccl20, Cd93, Ang1 and Ang2 and four factors were decreased; Tnfrsf11b, Csf2, Icam1 and Ccl17 (Figure 3B and Supplementary Figure 4B). Media was also harvested from tumours cells cultured alone but no changes in cytokine secretion were observed between control and mcoEltd1 expressing cells (data not shown).

To establish the source of cytokine secretion upon co-culture, the experiment was repeated and the cells harvested after 48 hours and separated into 4T1 tumour cells (GFP+) and sEnd.1 endothelial cells (GFP-) by FACs sorting. RNA was extracted from the cells and QPCR was performed to quantify the altered cytokines. mcoEltd1 was only significantly enriched in the 4T1-GFP-mcoEltd1 cell population confirming the efficient FACs sorting of the cells (Supplementary Figure 4C). Cd93, Ang1, Ang2 and Icam1 RNA expression was higher in endothelial cells. Il23, Tnfsr11b, Csf2, Ccl17 and Ccl20 levels were much higher, 10 fold or more, in tumours cells and are therefore the likely sources of secretion detected on the Cytokine Array (Figure 3C-D and Supplementary Figure 4C). Only Ccl17 and Ccl20 had changes at the RNA expression level that reflected the differences in protein secretion. Ccl20 expression levels were similar in 4T1-GFP-Control and 4T1-GFP-mcoEltd1 cells when they were cultured alone but its expression was significantly increased only in 4T1-GFP-mcoEltd1 cells when co-cultured with mouse endothelial cells (Figure 3C). Interestingly Ccl20 expression was also increased in the endothelial cells when co-cultured with the 4T1 cells, although much lower. (Figure 3C). Ccl17 was also increased in endothelial cells after co-culture with either cell line. (Figure 3D). Ccl17 expression was higher in control tumour cells when they were cultured with endothelial cells and increased upon co-culture in both tumour cell lines. However, overall there was lower Ccl17 expression levels in mcoEltd1 expressing cells compared to the control (Figure 3D).

4T1-mcoEltd1 tumours have altered leukocyte infiltration

To further investigate the changes in immune response *in vivo*, 4T1 control and 4T1-mcoEltd1 tumours were dissociated at endpoint and their immune cell infiltrate was profiled by FACS analysis. Both control and mcoEltd1 tumours had a significant percentage of leukocyte infiltration (CD45+ cells), that averaged 57.5% and 54.3% of the total tumour cell population respectively (Figure 4B). The major immune population in the tumour was myeloid cells (CD11b+), but there was no significant difference in overall number of cells between the groups (Figure 4B).

Next, we evaluated the frequency of specific immune cell subpopulations derived from the myeloid and lymphoid lineages of the blood, that could migrate to the tumour tissue. The Supplementary Figure 5 outlines the gating strategy for the analysis of immune cell infiltration. 4T1-mcoEltd1 tumours had an increase in the myeloid subsets that contain myeloid-derived suppressor cells (MDSCs): the Ly6G+ Ly6C^{low} population and Ly6C^{high}

ly6G^{low} monocytes population (Figure 4A and 4C)). The frequency of tissue macrophages with an M2-like phenotype, expressing F4/80 and CD206 (Figure 4A and 4D) was also increased in 4T1-mcoEltd1 tumours. Furthermore, a significant decrease in neutrophils and cytotoxic T cells was observed in 4T1-mcoEltd1 tumours when compared to the control tumours (Figure 4A and 4E). CD4^{+} T and B cell numbers were similar between the two groups (Figure 4A).

Programmed death-ligand 1 (PD-L1) expression is increased in mcoEltd1 tumours

PD-L1 is expressed on immune cells and a wide variety of tumour cells including breast, melanoma and lung, where it plays an important role in immune escape (15). We therefore analysed its level of expression on tumour cells and immune cell infiltrates using FACS. PD-L1 expression was significantly increased on 4T1-mcoEltd1 tumour cells (CD45-), leukocytes (CD45+) and mainly on the myeloid cell population (CD45+CD11b+) by 2.1, 2.4 and 2.5fold respectively (Figure 4F–H). Supplementary Figure 5 outlines the gating strategy for these experiments.

Spleen immune cell populations are altered in 4T1-mcoEltd1 tumour bearing mice

Spleens were also harvested from the 4T1 tumour growth study and the cells analysed by FACS. An increase in the myeloid cell population (CD11b+) in 4T1-mcoEltd1 tumour bearing mice was observed when compared to the controls. But unlike in the tumours, the monocytic Ly6C^{high} Ly6G^{low} population was lower in the 4T1-mcoEltd1 tumour bearing mice (Supplementary Figure 6A and D). Other changes in populations included a reduction in the neutrophil population, the dendritic cells, CD4^{+} T, CD8^{+} T-cell and NK cells in 4T1-mcoEltd1 tumour bearing mice with no significant changes in macrophage and B cell populations (Supplementary Figure 6A, E, F, G and H).

Expression of mcoEltd1 supresses the immune mediated rejection of NY-ESO-1 expressing tumours

We then analysed the impact of mcoEltd1 expression on the generation of specific immune T cell responses against the tumour. We used the antigen NY-ESO-1 (Cancer/testis antigen 1B), which is expressed in various types of tumour but not in healthy normal tissue (except in immune-privileged sites such as germ cells of the testis) and whose expression induces strong cellular and humoral immune responses(16). 4T1-NY-ESO-1 cells that also expressed mcoEltd1 and the relevant controls were implanted in BALBc WT mice and tumour growth was monitored. As previously shown, mcoEltd1 expression improves 4T1 tumour growth (Supplementary Figure 3C) and this effect was also retained when the NY-ESO-1 is co-expressed. However, when this antigen is expressed in control tumours (mcoEltd1^{-}/NY-ESO-1^{+}) they start regressing after approximately 12 days (Figure 5A and B), while the growth of the 4T1-NY-ESO-1-mcoEltd1 tumours was only slightly slower than mcoEltd1 tumours (not expressing NY-ESO-1) and did not show any sign of regression. The experiment was terminated after 21 days and, as the mcoEltd1 had continued to grow, they were significantly larger than the controls (Figure 5A and B).

The spleens were then harvested and the cells counted. Healthy non-tumour bearing mice were also used as a negative control. 4T1-NY-ESO-1-mcoEltd1 tumour bearing mice had

significantly more splenocytes compared to the controls (Figure 5C) but an equal number of active T CD8 cells (Figure 5D).

To test for the presence of activated T cells generated against the NY-ESO-1 antigen, we performed an IFNγ assay, where 10^6 splenocytes were stimulated with NY-ESO-1 peptide or an irrelevant peptide control (Flu NP) (or PMA-ionomycin as a positive control) for 4hrs. The number of IFNγ producing cytotoxic T cells was quantified using flow cytometry (Supplementary Figure 7A). The gating strategy for identification of IFNγ secreting cells is shown in Supplementary Figure 7C-H. There was no significant change in IFNγ production in response to the control peptide but a significant increase in activated T cells in response to the NY-ESO-1 peptide stimulation in mice with control tumour compared with mice bearing the mcoEltd1 tumour (Supplementary Figure 7B). The levels of IFN-γ produced by the NY-ESO-1 stimulated cells was very low compared with IFN-γ produced by stimulation with PMA-ionomycin (a stimulation that is not specific to any antigen). As expected, in all mice a significant proportion of $CD8^+$ were capable of IFNγ production following non-specific stimulation, using PMA-ionomycin, thus demonstrating the validity of the assay (Supplementary Figure 7B).

Primary breast cancer tumour cells can express ELTD1 and high expression correlates with better relapse free survival (RFS)

ELTD1 IHC was performed on primary human breast cancer core biopsies from 278 patients with matched survival data. The antibody used has been previously validated and published in Masiero et.al. 2013(4) and validated on the Protein Atlas (https://www.proteinatlas.org/). An example of antibody specificity is shown in Supplementary Figure 8A. Patient characteristics are shown in Supplementary Table 2. The intensity of tumour staining was scored (0=negative, 1=low, 2=moderate, 3=high; representative scoring in Figure 6A) and 35% had positive tumour staining with 9% (n=24) having high expression (IHC score 2-3) correlating with a better RFS (Figure 6B and 6C). Staining of 43 primary and matched involved lymph axillary nodes samples from a different patient cohort revealed that 51% of the primary breast tumours were positive for ELTD1 (16% having high expression; n=7), compared to 53% of the secondaries (12% high expression, n=5) (Figure 6D). There was no differential expression in tumour cell ELTD1 between primary breast tumours and their matched nodal metastases (Figure 6E). Of the small number of patients with high level tumour cell ELTD1 expression (IHC score 2-3), most only had high expression in either the primary or metastatic node, but not both (Figure 6F). The patient characteristics of the matched samples are shown in Supplementary Table 2.

ELTD1 expression in breast cancer vessels also correlates with better RFS

Vascular ELTD1 expression was scored in the 278 breast cancer samples (examples of staining and scoring shown in Supplementary Figure 8B). As with tumour expression, high ELTD1 tumour vessel expression correlated with a better RFS (Supplementary Figure 8C). In the paired samples, there was significantly higher expression of ELTD1 in tumour vessels compared to normal vessels in both the primary and secondary tumours (Supplementary Figure 8D). There was no differential expression in the normal vessels between the primary

and secondary samples whilst tumour vessel ELTD1 expression was slightly decreased in the regional nodal metastases (Supplementary Figure 8D).

There was no OS association for either tumour vessel or tumour cell ELTD1 expression (data not shown).

E0771-mcoEltd1 expressing tumours respond better to chemotherapy

E0771-mcoEltd1 tumours grew better *in vivo* and were better perfused compared to the controls (Figure 1). To investigate whether the tumours would respond better to chemotherapy, E0771 tumours were grown in C57BL/6 mice and treated with doxorubicin when tumours were palpable (approximately day 7). Untreated E0771-mcoEltd1 tumours became significantly larger than the controls at day 8 (Figure 7A and 7B) as previously observed. Doxorubicin treatment significantly decreased the growth of the control tumours but only at day 14 (Figure 7C). However, E0771-mcoEltd1 tumours were significantly more sensitive to treatment with reduced growth apparent as early as day 8 and a much greater effect by day 14 when compared to the controls (Figure 7D).

Discussion

ELTD1 is up regulated in breast cancer stroma(4) but expression in breast cancer tumour cells has not been previously reported. Staining of the primary breast cancer core biopsies and primary and matched involved lymph axillary nodes samples revealed not only vessel staining but also expression by tumour cells. It is unclear what triggers tumour ELTD1 expression *in vivo* and *in vitro*, we cannot detect the ELTD1 protein in breast tumour cell lines. ELTD1 has very poor codon usage and increasing the levels of its transcript in tumours cells does not lead to an increase in protein levels, which suggests a tight regulation at the translational level (data not shown)(12). ELTD1 may be a translated under certain stress conditions and rapidly synthesised by stress-induced pools of tRNAs(17). Stresses that occur in the tumour microenvironment include hypoxia, low pH, elevated interstitial fluid pressure and increased stiffness and warrant further investigation(18).

To induce protein expression of Eltd1 we had to codon optimise the mouse Eltd1 sequence to enable us to study the interaction of these tumour cells with mouse stroma in an immune competent environment. McoEltd11 expression in E0771 and 4T1 cells had no significant effect on tumour cells *in vitro* but significantly increased the growth of both cell lines tumours *in vivo*.

The tumours were better perfused and had decreased hypoxia and necrosis. Vessels were significantly larger in mcoEltd1 expressing tumours compared to the controls and had better pericyte coverage, suggesting that enhanced vessel function and/or vascular normalisation(19) may be the primary cause of the increased tumour growth.

Adhesion GPCRs are thought to act through cell-cell interaction and endothelial cells endogenously express ELTD1, especially in tumour vasculature(4,11). Tumour cells expressing mcoEltd1 grew faster when co-cultured with endothelial cells, especially when they physically contacted, and there were changes to the expression and/or secretion of

a number of cytokines that can influence angiogenesis and the immune system. The expression and secretion of Ccl20 was significantly increased in mcoEltd1 expressing tumour cells only after endothelial cell co-culture. Ccl20 could be involved in creating the phenotype observed in the mcoEltd1 tumours as it has been shown to promote cancer progression by increasing the proliferation of tumour cells. It also modulates the tumour microenvironment by promoting the infiltration of tumour associated macrophages (TAMs) and by the induction of angiogenesis (20). Another candidate factor is Il23 as there was a greater than two-fold increase in secretion, but not expression, of this cytokine when mcoEltd1 cells were co-cultured. This cytokine can also increase tumour cell proliferation and inhibit anti-tumour immune responses by reducing CD4+ and CD8+ T-cells in the tumour microenvironment as well as increasing M2-macrophage and neutrophil infiltration (21,22). Other factors that were increased only at the level of secretion in response to mcoEltd1 expression were Ang1 and 2 and soluble Cd93(23,24). These are pro-angiogenic and mainly expressed in the mouse endothelial cells. The secretion of a number of cytokines were decreased in mcoEltd1 expressing tumour cells after co-culture, all of which have some role in the immune response (20,25,26), these were also predominately expressed in the tumour cell lines. One of these, Ccl17, was also decreased at the RNA level when mcoEltd1 was expressed in 4T1 cells and after co-culture with endothelial cells. Ccl17 can recruit cytotoxic T cells and help activate CD8+ T cells (27) therefore a reduction of this cytokine in mcoEltd1 xenografts could reduce the anti-tumour immune response.

Inflammation is also a hallmark of cancer(28) and tumours are known to contain large numbers of myeloid cells which facilitate tumour growth and metastasis(29). 4T1 control and mcoEltd1 tumours both had a large infiltration of myeloid cells but 4T1-mcoEltd1 tumours had a greater percentage of M2 macrophages, (qPCR measurements of genes that are induced in M2 macrophages (Arg1, Mrc1 and Fizz) were also higher in mcoELTD1 expressing tumours). Macrophages were divided into M1 (classically activated) and M2 (alternatively activated) phenotypes(30) though there is much greater heterogeneity. Nevertheless, most data is still classified in this way. M1 macrophages accumulate at sites of chronic inflammation and in early tumours but then switch to immunosuppressive M2-like macrophages (also known as TAMs), as the tumour progresses(31–33). Therefore, expansion of these population, as has been noted in mcoEltd1 expressing tumours, is likely to have a suppressive impact on anti-tumour immune responses.

Immune cell function in tumours is heavily regulated by a series of checkpoint pathways(34). Among these, one of the better understood and clinically relevant, is the interaction between PD-1 and its ligand PD-L1(35). PD-L1 levels were also increased on the surface of tumour cells and on infiltrating leukocytes and myeloid cells in the 4T1-mcoEltd1 tumours compared to the controls.

Anti-tumour immunity is also regulated by key cell populations, such as MDSCs that have an important immune-suppressive function (36). mcoEltd1 expressing tumours contained higher ratio of $Ly6G^{high}L6C^{low}$ and $Ly6C^{low}Ly6C^{high}$ cells, both of which contain Myeloid Derived Suppressor Cells (MDSC)(37). The mechanisms by which MDSC suppress are varied but it is worth noting that one of the mechanisms involves expression of the enzyme arginase which depletes local concentrations of arginine which limit the function of immune

effector cells. qPCR measurements revealed higher levels of arginase gene expression in bulk tumour tissue from coELTD1 expressing tumours. There was also a reduction in cytotoxic T cell numbers.

The microenvironment of 4T1-mcoEltd1 was inferred to be functionally more immunosuppressive using NY-ESO-1 expressing tumour cells. Response to this well-defined tumour antigen could then be compared and effects of Eltd1 analysed, which was not possible in other *in vivo* studies reported(6,7). CD8+ T cells isolated from the spleens of animals implanted with Eltd1^{+} tumour cells were less responsive to the NY-ESO-1 peptide and the tumours were able to escape the immune mediated rejection observed in the absence of Eltd1 expression.

Tumours can display systemic effects on immune cell populations, modulating the response even before the immune cells reach the tumour microenvironment(38). Il-23 can influence the production of inflammatory cytokines in spleens during tumour development and may be involved in changing the spleen cell populations after mcoEltd1 tumour expression(39,40).

Increased metastasis was also present in the lungs of mice with 4T1-mcoEltd1 primary tumours when compared to the controls. Angiogenesis is important in metastasis and the larger, better perfused vessels produced by 4T1-mcoEltd1 tumours could be enhancing tumour cell dissemination(41). However, for metastasis to occur, tumour cells not only need angiogenesis but also the ability to detach from the primary tumour (intravasation) and invade through endothelial junctions (extravasation)(41). We found no differences in the invasiveness of E0771 or 4T1-mcoEltd1 cells in *vitro* but experiments using I.V. injection of mcoEltd1 tumour cells directly into the bloodstream also led to an increase in lung metastasis. This suggests that mcoEltd1 expressing tumour cells have an increased ability to metastasize and grow *in vivo* beyond intra- and extravasation at the primary site. Angiogenesis and immune suppression are factors that influence not only growth at the primary tumour site, but play an important role also in the metastatic niche. Therefore Eltd1's role in these processes may be important in priming the lung for secondary tumour growth and also enabling a better growth of a formed metastasis(42). ELTD1's presence in plasma was noted in older studies and in the metastatic niche(43,44).

ELTD1 expression has also been described in primary tumour cells of head and neck, renal, colorectal, glioblastoma and hepatocellular cancers, with expression correlating to a good prognosis in hepatocellular carcinoma and a poor prognosis in glioblastoma(6,7). We found that approximately 9% of breast tumours expressed high ELTD1 levels and this expression correlated with a better relapse free survival (RFS). High ELTD1 expression is also associated with the vasculature of renal, ovarian, head and neck, colorectal and hepatocellular carcinomas and this correlates with a good prognosis when the patient is undergoing anti-cancer treatments(4,6). We have previously shown that *ELTD1* RNA levels are increased in breast cancer stroma compared to normal stroma (4) and we can now confirm this at the protein level after performing IHC on 278 breast cancer biopsies.

Superficially, the clinical data does not appear to fit with our *in vivo* findings, with the first supporting a good prognostic value and the second demonstrating a clear and multifaced

pro-tumour function. However, it is worth remembering that patients had all undergone some form of cancer treatment where enhanced drug delivery or oxygenation could play a role. Therefore, higher ELTD1 levels could enhance tumour growth but at the same time make it more sensitive to drug treatment, as we showed here for doxorubicin.

A similar concept is behind the idea that anti-angiogenic therapies have the ability to induce “vascular normalisation” and create vessels that are more capable of delivering anti-cancer therapies as well as reducing the rate of metastasis(45). Unfortunately, inhibitors of the VEGF pathway only create a “window” of normalisation during which combination therapy can be used(46). Activation of the Tie2 pathway induced a more stable tumour vascular normalisation, leading to enhanced blood perfusion and effective drug delivery to reduce tumour growth and metastasis(47). Activation of ELTD1 could induce a similar phenotype. Vascular normalization improves immunotherapy if it is associated with an increase in perfusion(48). Therefore, immune checkpoint inhibitors such as anti–PD-1/anti–PD-L1 may be more effective in high ELTD1 expressing tumours, as well as other therapeutic regimes such as radiotherapy and chemotherapy. In conclusion ELTD1 elicits a complex response in tumour and stroma producing pro-angiogenic and immune suppressive effects. It will be of interest to investigate this in future studies, and to develop approaches to target ELTD1 in combination with conventional therapies.

Supplementary Material

Refer to Web version on PubMed Central for supplementary material.

Sources of Funding

This work was funded by Cancer Research UK (Project no. C602/A18974) and the Breast Cancer Research Foundation (Grant 2020).

Financial support

This work was funded by Cancer Research UK (Project no. C602/A18974) and the Breast Cancer Research Foundation (Grant 2020).

References

1. Nechiporuk T, Urness LD, Keating MT. ETL, a novel seven-transmembrane receptor that is developmentally regulated in the heart. ETL is a member of the secretin family and belongs to the epidermal growth factor-seven-transmembrane subfamily. J Biol Chem. 2001; 276 :4150–7. [PubMed: 11050079]
2. Herbert JM, Stekel D, Sanderson S, Heath VL, Bicknell R. A novel method of differential gene expression analysis using multiple cDNA libraries applied to the identification of tumour endothelial genes. BMC Genomics. 2008; 9 :153. [PubMed: 18394197]
3. Wallgard E, Larsson E, He L, Hellstrom M, Armulik A, Nisancioglu MH, et al. Identification of a core set of 58 gene transcripts with broad and specific expression in the microvasculature. Arterioscler Thromb Vasc Biol. 2008; 28 :1469–76. [PubMed: 18483404]
4. Masiero M, Simoes FC, Han HD, Snell C, Peterkin T, Bridges E, et al. A core human primary tumor angiogenesis signature identifies the endothelial orphan receptor ELTD1 as a key regulator of angiogenesis. Cancer Cell. 2013; 24 :229–41. [PubMed: 23871637]

5. Serban F, Artene SA, Georgescu AM, Purcaru SO, Tache DE, Alexandru O, et al. Epidermal growth factor, latrophilin, and seven transmembrane domain-containing protein 1 marker, a novel angiogenesis marker. Onco Targets Ther. 2015; 8 :3767–74. [PubMed: 26719704]
6. Kan A, Le Y, Zhang YF, Duan FT, Zhong XP, Lu LH, et al. ELTD1 Function in Hepatocellular Carcinoma is Carcinoma-Associated Fibroblast-Dependent. J Cancer. 2018; 9 :2415–27. [PubMed: 30026838]
7. Li J, Shen J, Wang Z, Xu H, Wang Q, Chai S, et al. ELTD1 facilitates glioma proliferation, migration and invasion by activating JAK/STAT3/HIF-1alpha signaling axis. Sci Rep. 2019; 9 13904 [PubMed: 31554859]
8. Ziegler J, Zalles M, Smith N, Saunders D, Lerner M, Fung KM, et al. Targeting ELTD1, an angiogenesis marker for glioblastoma (GBM), also affects VEGFR2: molecular-targeted MRI assessment. Am J Nucl Med Mol Imaging. 2019; 9 :93–109. [PubMed: 30911439]
9. Zalles M, Smith N, Ziegler J, Saunders D, Remerowski S, Thomas L, et al. Optimized monoclonal antibody treatment against ELTD1 for GBM in a G55 xenograft mouse model. J Cell Mol Med. 2019
10. Favara DM, Banham AH, Harris AL. A review of ELTD1, a pro-angiogenic adhesion GPCR. Biochem Soc Trans. 2014; 42 :1658–64. [PubMed: 25399586]
11. Hamann J, Hsiao CC, Lee CS, Ravichandran KS, Lin HH. Adhesion GPCRs as Modulators of Immune Cell Function. Handb Exp Pharmacol. 2016; 234 :329–50. [PubMed: 27832495]
12. Favara DM, Banham AH, Harris AL. ADGRL4/ELTD1 is a highly conserved angiogenesis-associated orphan adhesion GPCR that emerged with the first vertebrates and comprises 3 evolutionary variants. BMC Evol Biol. 2019; 19 :143. [PubMed: 31299890]
13. Williams RL, Risau W, Zerwes HG, Drexler H, Aguzzi A, Wagner EF. Endothelioma cells expressing the polyoma middle T oncogene induce hemangiomas by host cell recruitment. Cell. 1989; 57 :1053–63. [PubMed: 2736622]
14. Young YK, Bolt AM, Ahn R, Mann KK. Analyzing the Tumor Microenvironment by Flow Cytometry. Methods Mol Biol. 2016; 1458 :95–110. [PubMed: 27581017]
15. Kythreotou A, Siddique A, Mauri FA, Bower M, Pinato DJ. Pd-L1. J Clin Pathol. 2018; 71 :189–94. [PubMed: 29097600]
16. Raza A, Merhi M, Inchakalody VP, Krishnankutty R, Relecom A, Uddin S, et al. Unleashing the immune response to NY-ESO-1 cancer testis antigen as a potential target for cancer immunotherapy. J Transl Med. 2020; 18
17. Torrent M, Chalancon G, de Groot NS, Wuster A, Madan Babu M. Cells alter their tRNA abundance to selectively regulate protein synthesis during stress conditions. Sci Signal. 2018; 11
18. Yang LV. Tumor Microenvironment and Metabolism. Int J Mol Sci. 2017; 18
19. Carmeliet P, Jain RK. Principles and mechanisms of vessel normalization for cancer and other angiogenic diseases. Nat Rev Drug Discov. 2011; 10 :417–27. [PubMed: 21629292]
20. Chen W, Qin Y, Liu S. CCL20 Signaling in the Tumor Microenvironment. Adv Exp Med Biol. 2020; 1231 :53–65. [PubMed: 32060846]
21. Nie W, Yu T, Sang Y, Gao X. Tumor-promoting effect of IL-23 in mammary cancer mediated by infiltration of M2 macrophages and neutrophils in tumor microenvironment. Biochem Biophys Res Commun. 2017; 482 :1400–6. [PubMed: 27956175]
22. Langowski JL, Zhang X, Wu L, Mattson JD, Chen T, Smith K, et al. IL-23 promotes tumour incidence and growth. Nature. 2006; 442 :461–5. [PubMed: 16688182]
23. Fagiani E, Christofori G. Angiopoietins in angiogenesis. Cancer Lett. 2013; 328 :18–26. [PubMed: 22922303]
24. Lugano R, Vemuri K, Yu D, Bergqvist M, Smits A, Essand M, et al. CD93 promotes beta1 integrin activation and fibronectin fibrillogenesis during tumor angiogenesis. J Clin Invest. 2018; 128 :3280–97. [PubMed: 29763414]
25. Hong IS. Stimulatory versus suppressive effects of GM-CSF on tumor progression in multiple cancer types. Exp Mol Med. 2016; 48 e242 [PubMed: 27364892]
26. Semmling V, Lukacs-Kornek V, Thaiss CA, Quast T, Hochheiser K, Panzer U, et al. Alternative cross-priming through CCL17-CCR4-mediated attraction of CTLs toward NKT cell-licensed DCs. Nat Immunol. 2010; 11 :313–20. [PubMed: 20190758]

27. Xiong Y, Liu L, Xia Y, Wang J, Xi W, Bai Q, et al. Low CCL17 expression associates with unfavorable postoperative prognosis of patients with clear cell renal cell carcinoma. BMC Cancer. 2017; 17 :117. [PubMed: 28178948]
28. Hanahan D, Weinberg RA. Hallmarks of cancer: the next generation. Cell. 2011; 144 :646–74. [PubMed: 21376230]
29. Schmid MC, Varner JA. Myeloid cells in tumor inflammation. Vasc Cell. 2012; 4 :14. [PubMed: 22938502]
30. Martinez FO, Gordon S. The M1 and M2 paradigm of macrophage activation: time for reassessment. F1000Prime Rep. 2014; 6 :13. [PubMed: 24669294]
31. Ruffell B, Affara NI, Coussens LM. Differential macrophage programming in the tumor microenvironment. Trends Immunol. 2012; 33 :119–26. [PubMed: 22277903]
32. Mantovani A, Marchesi F, Malesci A, Laghi L, Allavena P. Tumour-associated macrophages as treatment targets in oncology. Nat Rev Clin Oncol. 2017; 14 :399–416. [PubMed: 28117416]
33. Olingy CE, Dinh HQ, Hedrick CC. Monocyte heterogeneity and functions in cancer. J Leukoc Biol. 2019; 106 :309–22. [PubMed: 30776148]
34. Waldman AD, Fritz JM, Lenardo MJ. A guide to cancer immunotherapy: from T cell basic science to clinical practice. Nat Rev Immunol. 2020; 20 :651–68. [PubMed: 32433532]
35. Chen J, Jiang CC, Jin L, Zhang XD. Regulation of PD-L1: a novel role of pro-survival signalling in cancer. Ann Oncol. 2016; 27 :409–16. [PubMed: 26681673]
36. Ostrand-Rosenberg S, Fenselau C. Myeloid-Derived Suppressor Cells: Immune-Suppressive Cells That Impair Antitumor Immunity and Are Sculpted by Their Environment. J Immunol. 2018; 200 :422–31. [PubMed: 29311384]
37. Youn JI, Nagaraj S, Collazo M, Gabrilovich DI. Subsets of myeloid-derived suppressor cells in tumor-bearing mice. J Immunol. 2008; 181 :5791–802. [PubMed: 18832739]
38. Russo V, Protti MP. Tumor-derived factors affecting immune cells. Cytokine Growth Factor Rev. 2017; 36 :79–87. [PubMed: 28606733]
39. Sieve AN, Meeks KD, Lee S, Berg RE. A novel immunoregulatory function for IL-23: Inhibition of IL-12-dependent IFN-gamma production. Eur J Immunol. 2010; 40 :2236–47. [PubMed: 20458705]
40. Caughron B, Yang Y, Young MRI. Role of IL-23 signaling in the progression of premalignant oral lesions to cancer. PLoS One. 2018; 13 e0196034 [PubMed: 29664967]
41. Bielenberg DR, Zetter BR. The Contribution of Angiogenesis to the Process of Metastasis. Cancer J. 2015; 21 :267–73. [PubMed: 26222078]
42. Liu Y, Cao X. Characteristics and Significance of the Pre-metastatic Niche. Cancer Cell. 2016; 30 :668–81. [PubMed: 27846389]
43. Liu T, Qian WJ, Gritsenko MA, Camp DG 2nd, Monroe ME, Moore RJ, et al. Human plasma N-glycoproteome analysis by immunoaffinity subtraction, hydrazide chemistry, and mass spectrometry. J Proteome Res. 2005; 4 :2070–80. [PubMed: 16335952]
44. Niinivirta M, Georganaki M, Enblad G, Lindskog C, Dimberg A, Ullenhag GJ. Tumor endothelial ELTD1 as a predictive marker for treatment of renal cancer patients with sunitinib. BMC Cancer. 2020; 20 :339. [PubMed: 32321460]
45. Goel S, Wong AH, Jain RK. Vascular normalization as a therapeutic strategy for malignant and nonmalignant disease. Cold Spring Harb Perspect Med. 2012; 2 a006486 [PubMed: 22393532]
46. Winkler F, Kozin SV, Tong RT, Chae SS, Booth MF, Garkavtsev I, et al. Kinetics of vascular normalization by VEGFR2 blockade governs brain tumor response to radiation: role of oxygenation, angiopoietin-1, and matrix metalloproteinases. Cancer Cell. 2004; 6 :553–63. [PubMed: 15607960]
47. Park JS, Kim IK, Han S, Park I, Kim C, Bae J, et al. Normalization of Tumor Vessels by Tie2 Activation and Ang2 Inhibition Enhances Drug Delivery and Produces a Favorable Tumor Microenvironment. Cancer Cell. 2016; 30 :953–67. [PubMed: 27960088]
48. Mpekris F, Voutouri C, Baish JW, Duda DG, Munn LL, Stylianopoulos T, et al. Combining microenvironment normalization strategies to improve cancer immunotherapy. Proc Natl Acad Sci U S A. 2020; 117 :3728–37. [PubMed: 32015113]

Europe PMC Funders Author Manuscripts

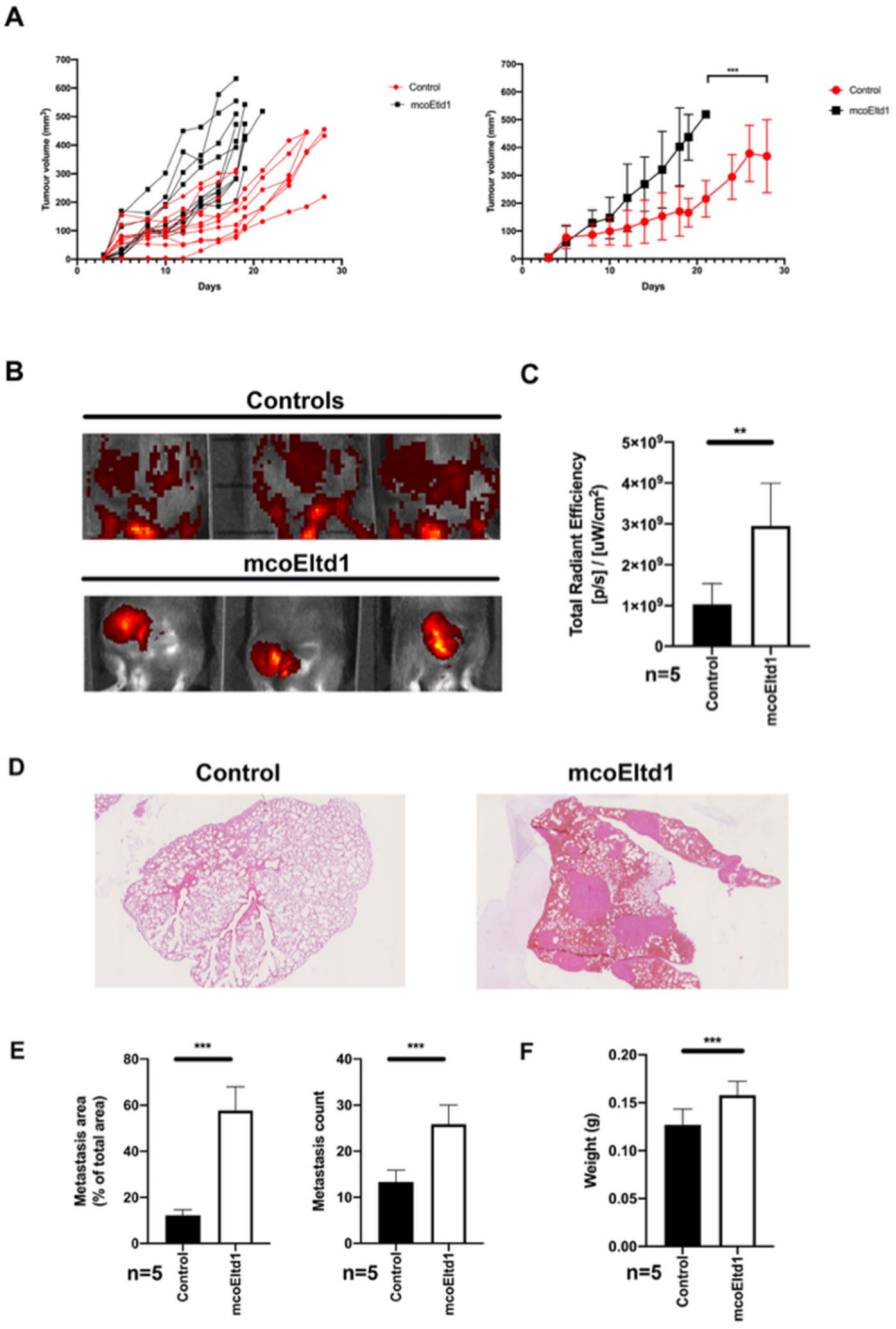

Figure 1. Expression of mcoEltd1 in breast tumours increases tumour growth and metastasis.

(A) Syngeneic tumour growth curves of E0771 control and E0771 mcoEltd1 tumours. Tumour sizes were compared at endpoint by un-paired *t*-test, n=8. Individual and merged graphs shown. **(B)** IVIS fluorescent imaging of perfused tumours and **(C)** quantification. **(D)** H&E staining of lungs collected at experiment end point. Representative images taken on a Nikon Eclipse E800 microscope at 4× magnification. **(E)** Quantification of tumour area and tumour number in lungs. Data analysed by un-paired *t*-test. **(F)** Weight of lungs at experiment end point. *p <0.05; **p <0.005; ***p <0.0005. n=5 biological replicates.

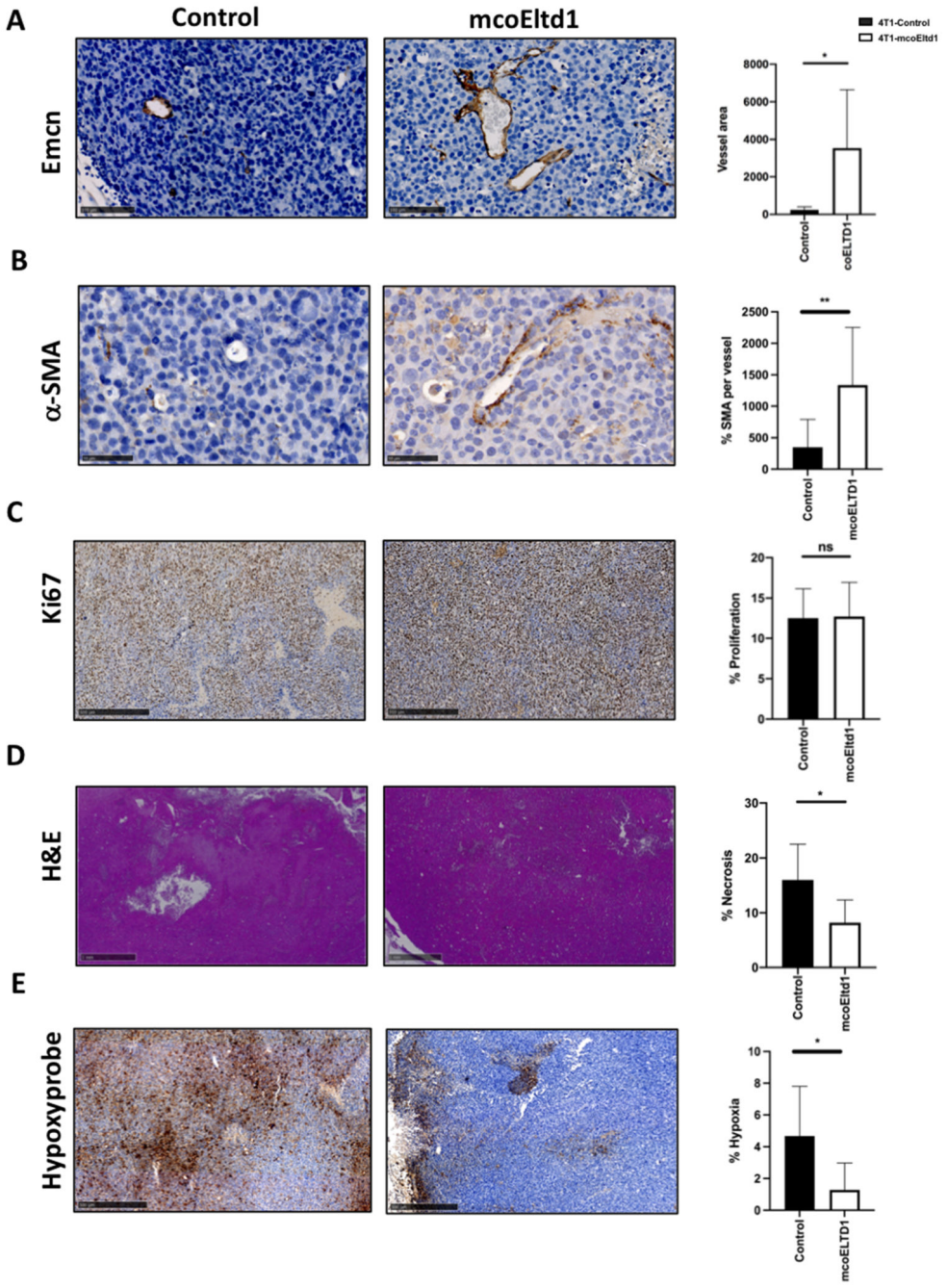

Figure 2. Eltd1 expression in tumours increases vessel size and decreases hypoxia.

Representative immunohistochemistry and quantification of (**A**) Endomucin vessel staining, (**B**) a-SMA staining for pericyte coverage, (**C**) Ki67 proliferation, (**D**) H&E Staining for necrosis, (**E**) Hypoxyprobe staining for hypoxia. Data analysed by un-paired *t*-test *p <0.05; **p <0.005; ***p <0.0005. n=5 biological replicates.

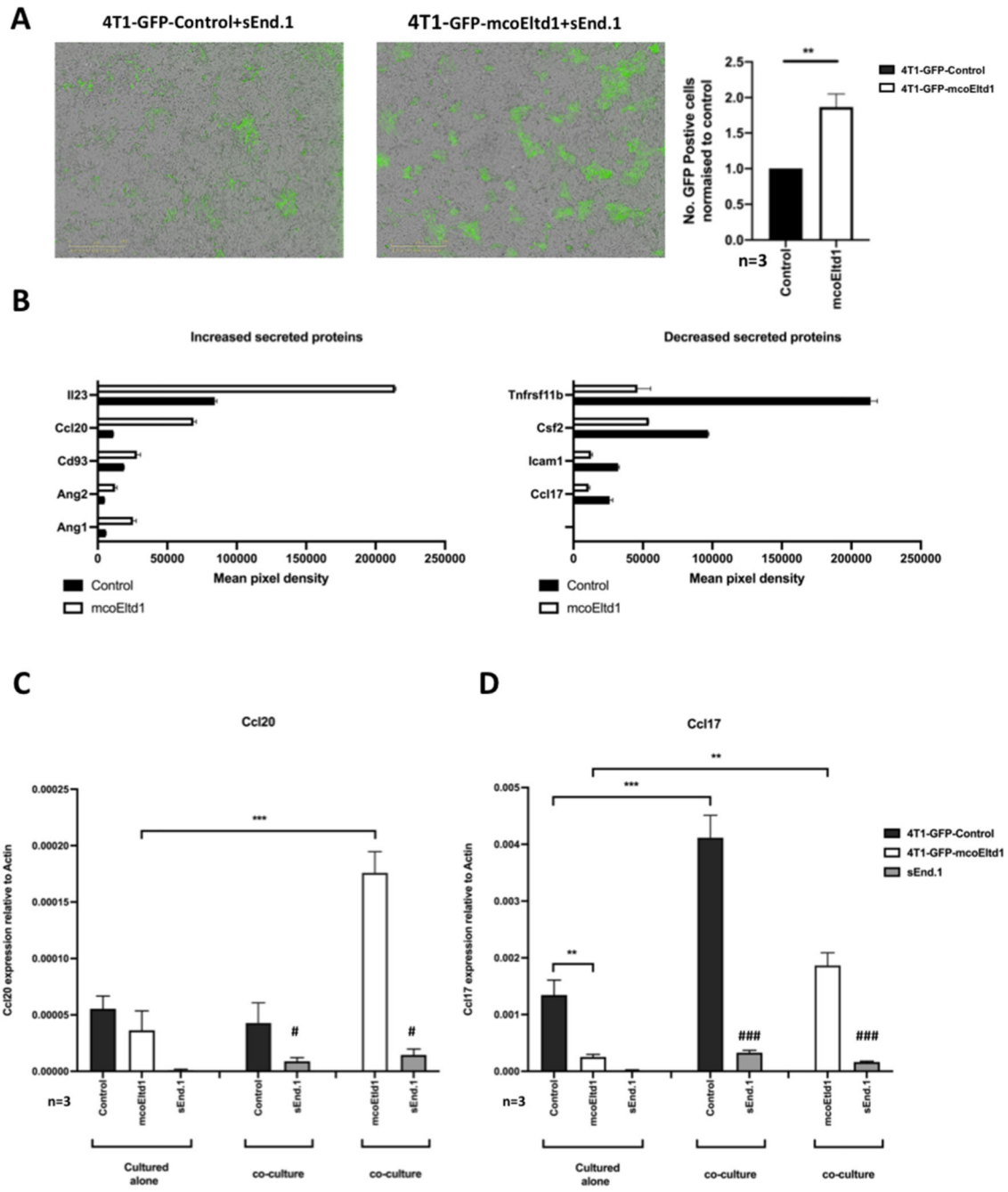

Figure 3. Eltd1 expressing tumour cells proliferate in the presence of endothelial cells and modifies their secretome.

(**A**) Appearance of 4T1 tumour cells (GFP positive) when co-cultured with mouse endothelial cells for 48hrs at 4x magnification and quantification of GFP positive cells (**B**) Quantification of a mouse cytokine array performed using the cell supernatants collected after 48hrs of co-culture. Dot intensity was quantified using Fiji software. (**C**) QPCR of Ccl20 and (**D**) Ccl17 from RNA extracted from mouse endothelial cells (sEnd.1) and 4T1 tumour cells cultured alone or after co-culture and subsequent FACs sorting. Data were

Europe PMC Funders Author Manuscripts

analysed by the unpaired *t*-test *p <0.05; **p <0.005; ***p <0.0005. # p <0.05, ### p <0.0005

Europe PMC Funders Author Manuscripts

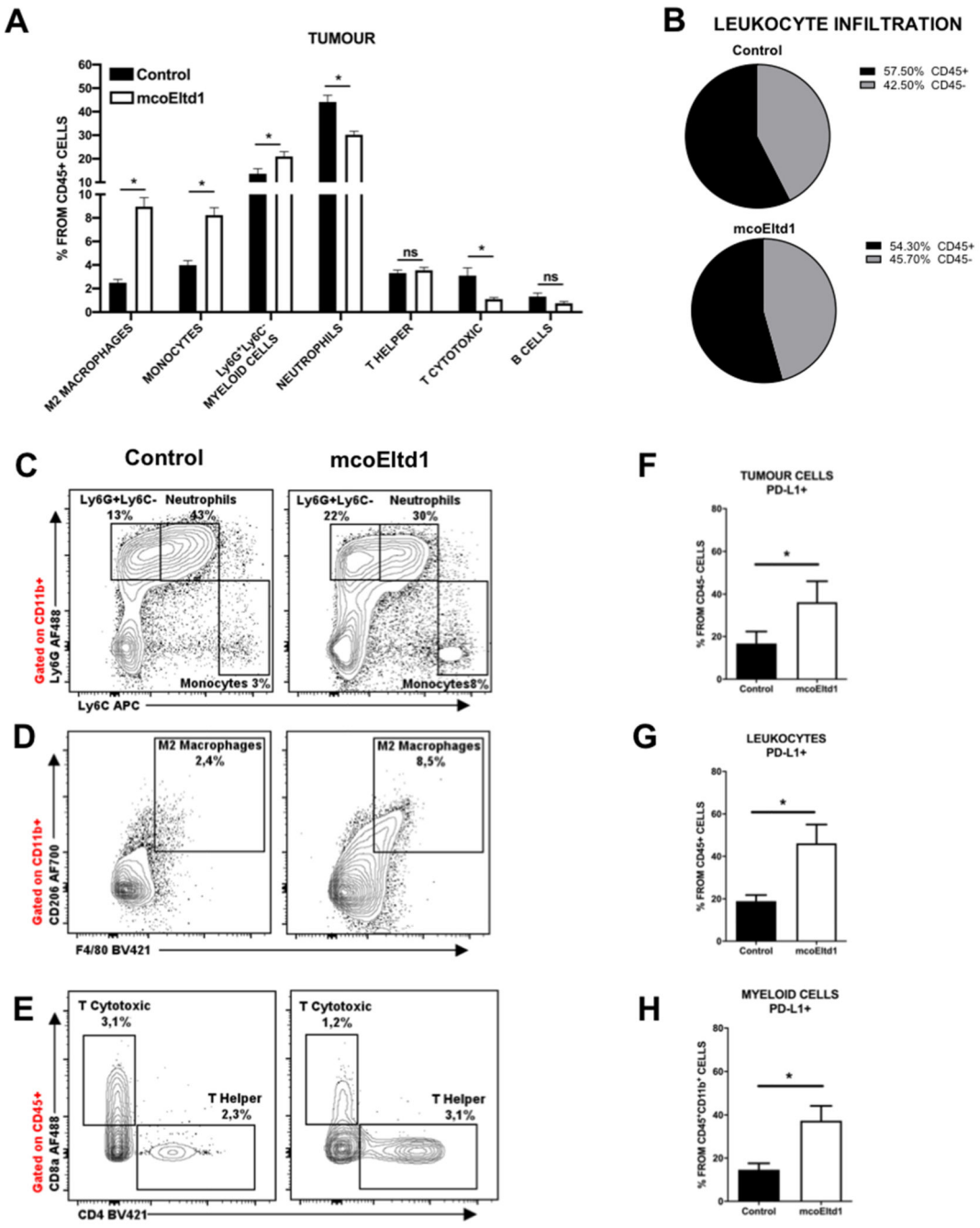

Figure 4. Eltd1 expression alters immune infiltration and PD-L1 expression within 4T1 tumours.

FACS analysis of the tumour cell populations at day 22 (**A**). Data are presented as mean percentage of CD45+ cells. (**B**). Pie charts represent the proportion of $CD45^{+}$ (all leukocytes) and $CD45^{-}$ (tumour cells and others) from the tumours. Representative scatter plots showing the differences in leukocyte populations within the tumour, (**C**). $Ly6G^{+}Ly6C^{-}$ Myeloid cells, Neutrophils, Monocytes (**D**), M2 Macrophages (**E**) CD4+ and CD8+ lymphocytes. Percentage PD-L1 expression in (**F**) tumour cells, (**G**) leukocytes, (**H**)

myeloid cells. Data analysed by the unpaired *t*-test (n=10 independent tumour samples analysed) *p <0.05.

Europe PMC Funders Author Manuscripts

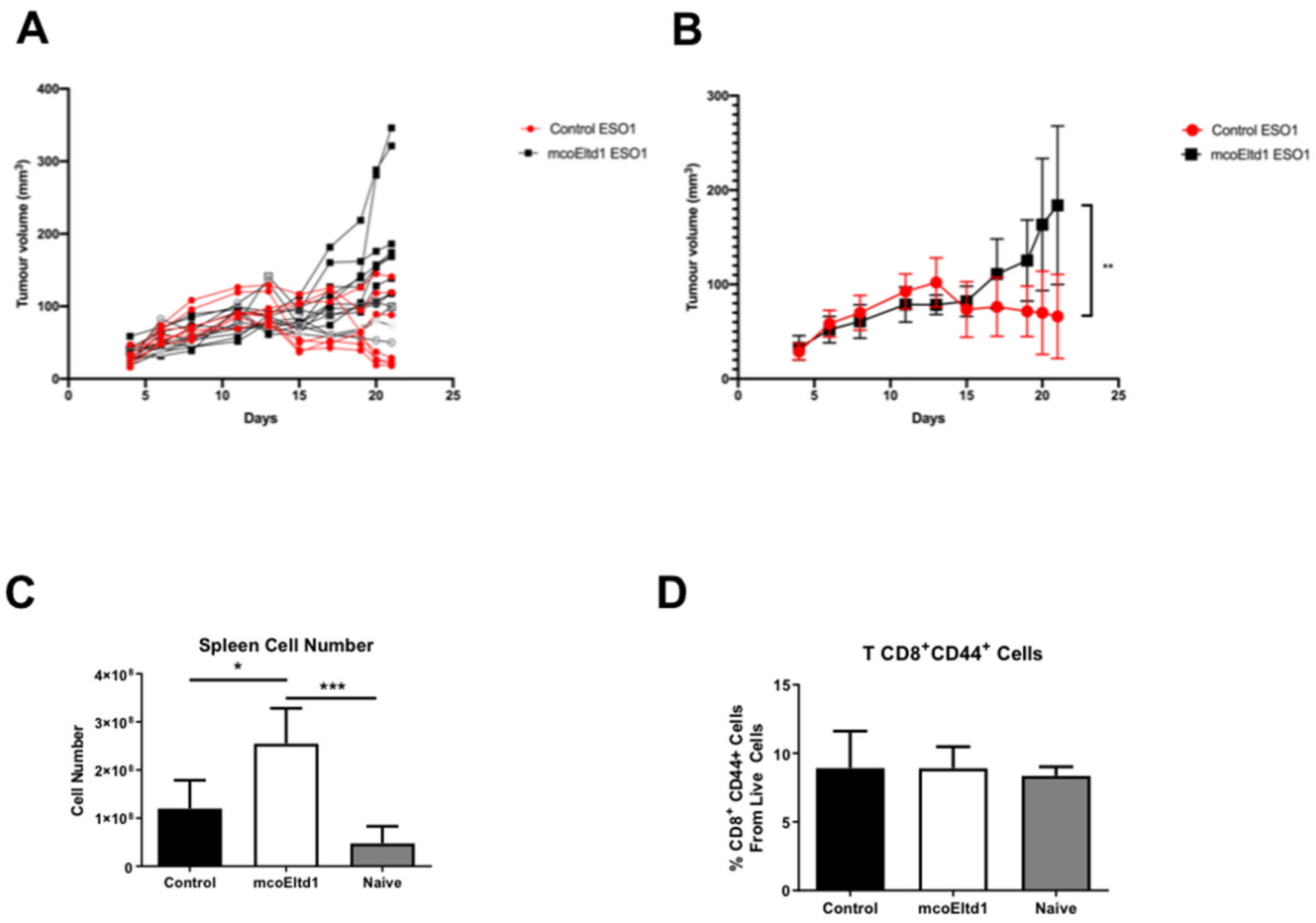

Figure 5. Expression of Eltd1 supresses the immune mediated tumour cell rejection of NY-ESO-1.

(A) Individual growth curves for 4T1-NY-ESO-1 control and mcoEltd1 expressing tumours **(B)** Merged data. Tumour sizes were compared at endpoint by the unpaired *t*-test **(C)** Total number of immune cells in the spleen of the controls and mcoEltd1 tumour allografts at day 22. A group of naïve/healthy mice were used as control. **(D)** Mean percentage of total CD8+ CD44+ active T CD8 cells ± SEM. Data were analysed by the unpaired t-test (n = 5 independent mice analysed). Data were analysed by the unpaired *t*-test ($n = 5$ independent mice analysed) *$p < 0.05$; **$p < 0.005$; ***$p < 0.0005$.

Europe PMC Funders Author Manuscripts

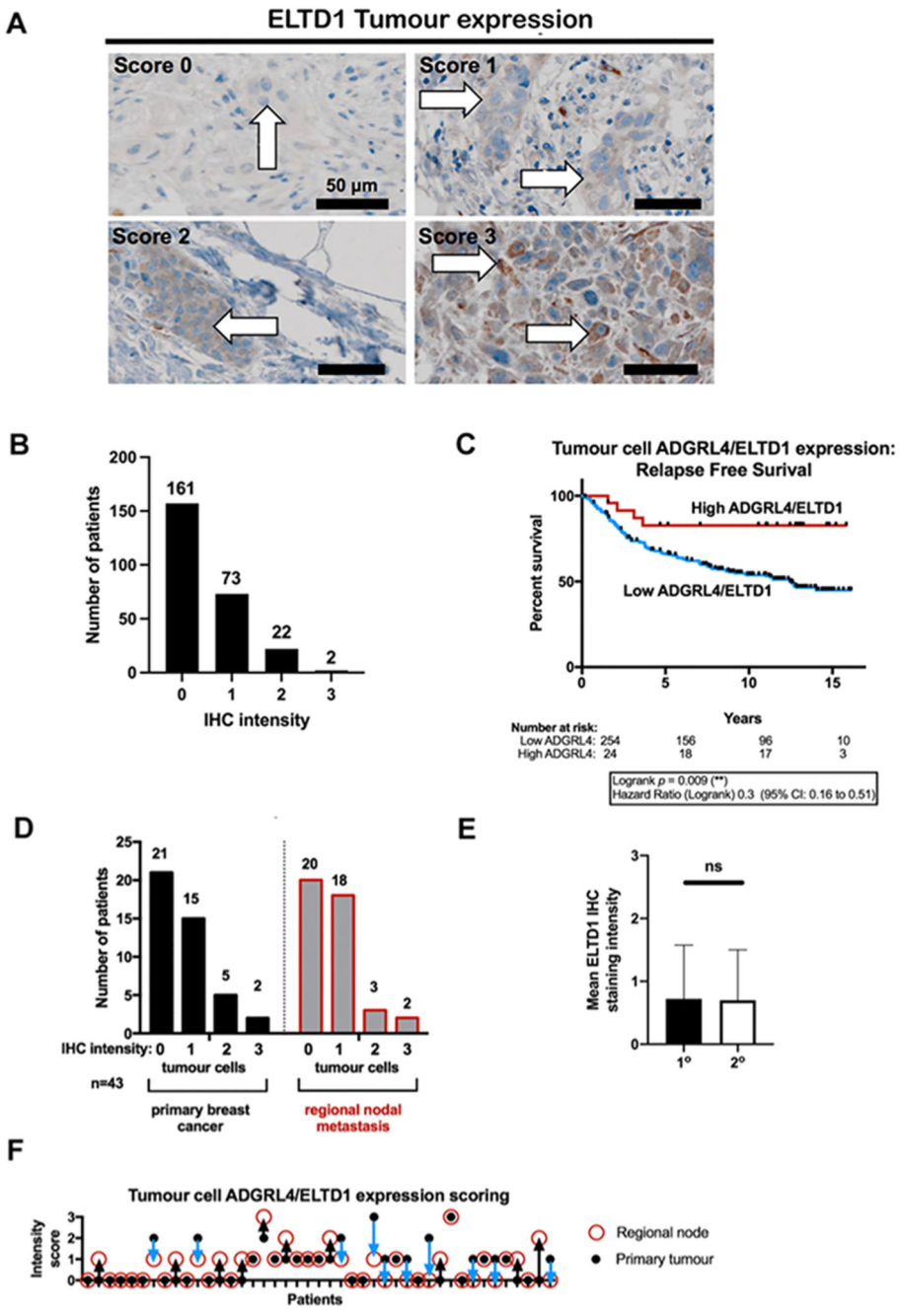

Figure 6. Breast cancer cells can express ELTD1 and high expression correlates with improved relapse free survival (RFS).

(A) Representative images of low (score 0) to high (score 3) tumour ELTD1 expression. **(B)** Histogram of tumour cell IHC expression in larger patient cohort **(C)** Survival plot showing improved RFS with higher tumour ELTD1 expression. **(D)** Histogram of tumour cell ELTD1 IHC expression in primary breast tumours and regional node metastases. **(E)** Comparison of tumour cell ELTD1 IHC expression between primaries and regional node metastases. Data analysed by un-paired *t*-test. **(F)** Tumour cell ELTD1 expression changes. Black arrows

Europe PMC Funders Author Manuscripts

indicate upward expression from primary tumour to metastatic node in the same patient; blue arrows indicate downwards expression in the same patient.

Europe PMC Funders Author Manuscripts

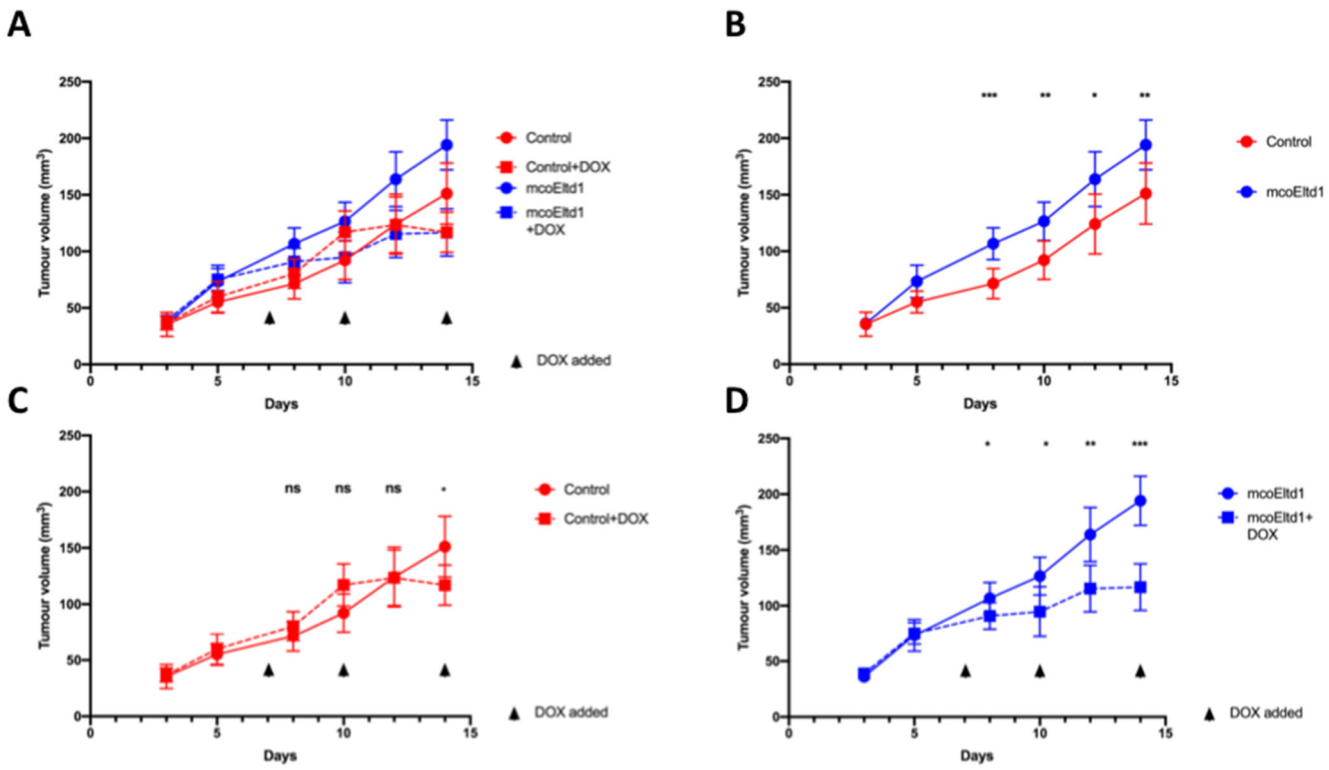

Figure 7. Eltd1 expressing tumours respond better to chemotherapy.

(**A**) Syngeneic tumour growth curves of E0771 control and E0771 mcoEltd1 tumours treated with or without doxorubicin (n=7). (**B**) Untreated tumour growth (**C**) Control +/− doxorubicin (**D**) mcoEltd1 +/− doxorubicin. Tumour sizes were compared between groups at day 8, 10, 12 and 15 and the data were analysed by the unpaired *t*-test **p* <0.05; ***p* <0.005; ****p* <0.0005.

Europe PMC Funders Author Manuscripts